Direct extraction of platinum nanoparticles from fuel cells with ionic liquids: Part 1. Implementation and optimization of the process parameters

Mathias Coudray, Emmanuel Billy, Hakima Mendil-Jakani, Paul Haumesser, Catherine C Santini, Véronique Dufaud

Direct extraction of platinum nanoparticles from fuel cells with ionic liquids: Part 1. Implementation and optimization of the process parameters

M. Coudray[a,b], E. Billy[c*], H. Mendil-Jakani[a], P.-H. Haumesser[d], C. C. Santini[b], V. Dufaud[b*]

[a] Univ. Grenoble Alpes, CEA, CNRS, INP, IRIG-SyMMES, 38000 Grenoble, France.

[b]University of Lyon, CPE Lyon, CNRS, UMR 5128, Catalysis, Polymerization, processes and Materials (CP2M), 43 Bd du 11 novembre 1918, F-69616 Villeurbanne cedex, France.

[c] Univ. Grenoble Alpes, CEA, LITEN, 17 rue des Martyrs, 38054 Grenoble, France.

[d] Univ. Grenoble Alpes, CEA, LETI, MINATEC Campus, 17 rue des Martyrs, 38054 Grenoble, France.

[*] Corresponding authors : Emmanuel.Billy@cea.fr; veronique.dufaud@univ-lyon1.fr

Abstract

The cost of proton-exchange membrane fuel cell (PEMFCs) comes mainly from the platinum nanoparticles, which are used as catalyst; it represents 40 % of the stack price for a large-scale production. It is thus crucial to reduce their cost to produce cheaper devices, which could compete with fossil energy on the industrial market. One way to reach this goal would be to recover the Pt catalyst from the membrane electrode assembly (MEA) for further recycling. For now, current end-of-life (EoL) technologies are mainly based on hydrometallurgical and pyro-hydrometallurgical processes for recovering platinum which are identified to be energy demanding generate high amounts of toxic liquids and gaseous effluents. To meet sustainability and circular economy criteria in the recycling of noble metals, our approach was based on the use of ionic liquids (ILs) to both extract and stabilize platinum in the form of metallic nanoparticles (Pt NPs), thus avoiding the emissions of hydrofluoric acid (HF) and the use of strong acids, which make the waste management of conventional processes complicated. Thirteen different ILs were selected to investigate

how their structural composition as well as their physico-chemical properties may affect the extent of Pt extraction, and their ability to stabilize detached nanoparticles. This screening study showed that ionic liquids could interact with all the elements of the active layer and allowed us to delineate the key parameters that ILs should possess to achieve the best extraction performance: hydrophilicity, the hydrogen bonding ability, the coordinating ability of the anions.

The best result was obtained with the trihexyltetradecylphosphonium chloride ($P_{66614}Cl$) (commercial Cyphos® IL 101) (120 °C and 6 h) which not only led to an extraction extent up to > 90 % of the Pt present initially on the catalytic layer, but also allowed in a single step to detach the Pt NPs from the carbon support. The metallic Pt NPs suspended in $P_{66614}Cl$ were found stable with diameter around 2-3 nm as evidenced by transmission electron microscopy (TEM) and high-resolution transmission electron microscopy (HRTEM) analyses. Compared to conventional processes, this safer and convenient route to recover Pt catalyst from MEAs directly in their metallic form by simple immersion of the electrode in the appropriate IL opens up new perspectives in term of rare earth metal recycling from material composites.

Keywords: fuel cells, platinum, recycling, ionic liquids, nanoparticles

I. Introduction

In order to significantly reduce our greenhouse gas emissions and our dependence to fossil energies, it is urgent to rapidly implement new alternative technologies capable of competing economically with heat engines with the aim of supplanting them within a 10 to 30 years' timeframe. One of the serious competitors to these engines is the fuel cell based on the use of dihydrogen produced by the electrolysis of water using electricity from renewable energies.(1)

Fuel cells are electrochemical devices that convert the chemical potential energy of a fuel (hydrogen gas) into electricity while yielding heat and water as the only reaction by-products. Among the fuel cell technologies, proton-exchange membrane fuel cells (PEMFC) are particularly suitable for electronics and automotive applications. The core of a PEMFC is the membrane electrode assembly (MEA) composed of : (i) a polymeric proton exchange membrane surrounded by (ii) two catalytic layers (CL), (iii) two microporous layers (MPL), and (iv) two gas diffusion layers (GDL).(2)

In PEMFC, platinum nanoparticles (Pt NPs: 2–5 nm) are considered as the current standard catalyst due to its good catalytic activity, stability to withstand the operating environment and resistance to corrosion.(3)

The catalytic reactions of hydrogen oxidation reaction (HOR) at the anode and oxygen reduction reaction (ORR) at the cathode are required at both electrodes containing the Pt catalyst, and can only occur at confined spatial sites, called "triple phase boundaries" where electrolyte, gas, and electrically connected catalyst regions are in close contact, (Scheme 1). The electrolyte also referred to as ionomer (typically a Nafion based polymer) acts as both proton conductor and binder and the carbon support ensures the electrical conductivity in the CL.

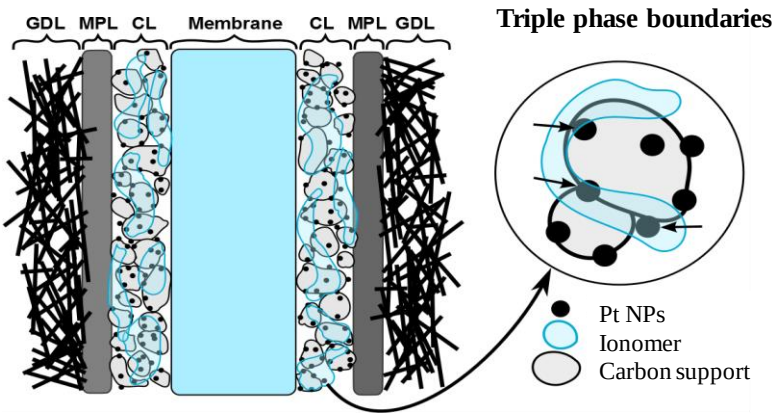

Scheme 1. The membrane electrode assembly (MEA) of a PEMFC.

The cost of PEMFCs comes mainly from the platinum catalyst, which represents ~ 40 % of the stack price for large-scale production. It is therefore crucial to reduce their cost to be able to produce cheap cells that could compete with fossil energy. It is also important to stress that, in the years to come; the supply of Pt will become a critical bottleneck owing to its very low availability in natural ores, which are to a large extent found in South Africa. Moreover, metallic platinum is one of the 83 critical raw materials (CRM) listed by the European Commission.(4) Therefore, to ensure reliable and stable Pt supply, the development of viable recycling processes for this metal that takes into account both environmental and economic issues is essential to allow for fuel cells intensification production at the industrial scale.

Current end-of-life (EoL) technologies applied to PEM systems combine a pyro-metallurgical and an hydrometallurgical process in which GDLs, membranes and electrodes are incinerated or calcined with emission of toxic and corrosive gas (such as hydrofluoric acid from Nafion), which causes severe safety and environmental concerns. The ashes resulting from the combustion are processed by dissolving them in a mixture of strong acids (aqua regia).(5) Finally, the soluble platinum is recovered by separation, by precipitation, solvent extraction (liquid-liquid extraction).(5-6) Another route consists in the electrochemical dissolution of platinum nanoparticles into Pt(II) in acidic media.(7-8)

Few reports have depicted the direct extraction of platinum in its metallic form from the different components of the catalytic layer. To our knowledge, only three patents more focused on ionomer recovery described the concomitant recovering of platinum metal. Their procedure is similar: separation of the membrane from the rest of the membrane electrode assembly constituents (swelling of the membrane), then the catalytic layer

consisting of Pt NPs supported on carbon black is dispersed within the solvent (alcohols, diols or supercritical liquids). In contact with Pt NPs, decomposition reactions of the solvents could occur causing auto-ignition in the presence of oxidizer, and therefore a risk of fire. In addition to these safety concerns, the removal of these organic solvents can be dangerous for the operator and his environment, and a source of additional expense for the company.(9-11)

Taken together, from academic and industrial literature, the current way to recover platinum from MEAs involves a pyro-hydrometallurgical process based on electrochemistry. The MEAs are first calcined to produce ashes that mainly contain metallic platinum which is converted into Pt(II) in aqueous acidic media whatever the nature of the solvent of extraction. Regardless of the process described above, platinum is mainly extracted in the form of divalent platinum requiring an additional step of controlled reduction to obtain Pt NPs of 2 nm in diameter for further use. As an alternative, liquid-based separation employing ionic liquids (hereafter abbreviated ILs) has emerged in the last years.(12)

ILs, salts in the liquid state**,** have been widely used as extractive solvent or directly as extractant due to the distinctive and unique properties they possess, such as negligible vapor pressure, wide solubility range, and flame-retardant property, as well as their tunable nature by simple variation of the building anions and cations.(13-14) In addition, in the field of recycling, mainly of platinum group metal catalysts (PGMs), ILs have been successfully used for the extraction of metal ions but also for the dissolution of metals from various solutions and supports.(15-19) Particularly, phosphonium-based ionic liquids have been reported to be effective candidates for the extraction and separation of PGMs.(20-24)

More recently, ILs have been shown to allow the electrochemical leaching of platinum by oxidation directly from the MEA without pyro-process and without IL degradation. The feasibility of this process is related to their relatively good ionic conductivities, and wide electro-chemical windows, typically greater than 2 V.(25) In addition, their wide electrochemical window could also allow for the recovery of metallic platinum by electrodeposition.(26-27)

A breakthrough in the greenness of Pt recycling from MEAs using ILs could be related to the following properties: i) the high wettability of carbon material (electrode, coal, graphite) by ILs.(28) Indeed, a range of imidazolium based ILs were capable of

disintegrating, dispersing and solubilizing a range of coal,(28-30) as well of exfoliating graphite at ambient temperature.(31-32) ii) The interaction between Pt NPs and carbon material based on dispersion forces (London forces) are rather weak interactions which makes possible NPs leaching.(33-36) iii) Moreover, it is widely reported in the literature that ILs have the ability to stabilize metal nanoparticles (MNPs) even smaller than 10 nm.(37-38) Even if these ILs are mainly based on imidazolium cations, other ILs derived from phosphonium cations have shown to enable very good stabilization of palladium NPs. It is widely accepted that ILs aggregates interact with metal NPs. Consequently, both the coordination properties of the anion, and/or the interactions with the cation and the hydrocarbon chains linked to phosphonium or imidazolium cation, are favorable elements for the separation of Pt NPs.(39-42)

The aim of this series of publications is to develop an innovative approach for the direct extraction of Pt NPs from MEA electrodes by ILs, thus avoiding the electrode calcination and platinum dissolution steps. ILs are non-flammable and non-volatile liquid salts stable up to 300 °C, which could allow the implementation of a safer process. Moreover, for sustainability, economic and waste management considerations, we designed a convenient one-step process for the recovery of Pt NPs by simply immersing the electrode in the ILs under appropriate reaction conditions.

In the first part of this work, we propose to concentrate on the macroscopic interactions between the ILs and the catalytic layer. For this purpose and in order to demonstrate the feasibility of a separation process, *i.e.* detach the Pt NPs from the CL while avoiding agglomeration of the extracted NPs, a large panel of ILs with varied cation/anion compositions and physicochemical properties was tested. Thus, a thorough screening of the ILs and operating conditions allowed us to delineate the key features ILs should possess as well as the best suitable operating conditions to achieve the best extraction performance. As described above, the CL is also composed of different components, notably Nafion used as a binder. The Nafion ionomer is known to swell in the presence of ILs.(43-49) This phenomenon is probably also involved in the leaching of Pt NPs and constitutes a study in itself which will be presented in detail in the second part of this series of publications for a better understanding of the extraction mechanism.

II. Experimental Section

Reference electrode. The electrodes used in this study consist of a catalytic layer (CL), containing platinum, deposited on a carbon paper based microporous layer (GDL) made of carbon black (Vulcan XC 72R) and dispersed Nafion, which acts as the binder. Several electrodes with different composition in terms of Pt loading, ionomer content and nature of the support have been studied (*vide infra*), however, for the ILs screening study, an home-made electrode supplied by CEA-LITEN (El_{REF}) with Pt loading close to that of commercial devices was used. Its principal characteristics are displayed in Table 1.

Table 1. Main characteristic of the reference electrode (El_{REF}).

Support	Pt (wt %)	Ionomer (I) (wt %)	Carbon (C) (wt %)	Pt/C (wt %)	I/C[a]	Loading (mg Pt.cm^{-2})	Thickness CL (μm)	Size Pt NPs (nm)	Size C particle (nm)
GDL	34.3	26.2	39.5	46.5	0.67	0.22± 0.03	~ 10	3.0 ± 0.6	15-50

[a] Weight ratio. The average thickness of the catalytic layer (CL) was measured by scanning electron microscopy (SEM), the Pt loading was determined by optical emission spectrometry with inductively coupled plasma (ICP-OES). The average diameters of platinum nanoparticles (Pt NPs) were measured by transmission microscopy (TEM) for at least 150 nanoparticles.

Selected ionic liquids. The ILs (Table 2) were purchased from Solvionic and/or from Iolitec with a purity of at least 98 %. They were used as received and stored under argon in a glove-box. Acetonitrile (ACN), dimethylsulfoxyde (DMSO), dimethylacetamide (DMAc), isopropanol, ethanol (99 %) were supplied from Sigma-Aldrich and used without further purification.

Table 2. Ionic liquids used in this work and nomenclature and safety sheet for $P_{66614}Cl$*

Cation	Anion	Abbreviation
1-ethyl-3-methylimidazolium	tricyanomethanide	C_1C_2ImTCM
1-butyl-3-methylimidazolium	bis(trifluoromethylsulfonyl)imide	$C_1C_4ImNTf_2$
1-butyl-3-methylimidazolium	trifluoromethanesulfonate	C_1C_4ImOTf
1-butyl-3-methylimidazolium	Dicyanamide	$C_1C_4ImN(CN)_2$
1-butyl-3-methylimidazolium	Acetate	C_1C_4ImAc
1-butyl-3-methylimidazolium	Chloride	C_1C_4ImCl
1-butyl-2,3-dimethylimidazolium	bis(trifluoromethylsulfonyl)imide	$C_1C_1C_4ImNTf_2$
N-tributyl-N-methylammonium	Dicyanamide	$N_{4441}N(CN)_2$
Trihexyltetradecylphosphonium	Dicyanamide	$P_{66614}N(CN)_2$
Trihexyltetradecylphosphonium	tricyanomethanide	$P_{66614}TCM$
Trihexyltetradecylphosphonium	Chloride	$P_{66614}Cl$*

Trihexyltetradecylphosphonium	Bromide	$P_{66614}Br$
Trihexyltetradecylphosphonium	bis(trifluoromethylsulfonyl)imide	$P_{66614}NTf_2$

*https://iolitec.de/sites/iolitec.de/files/sds/SDS%20IN-0006%20P666%2814%29%20Cl%2C%20Trihexyltetradecylphosphonium%20chloride.pdf

Pt extraction procedure. In a typical experiment (Figure 1), an electrode sample of 3 x 6 mm size was immersed over a length of 4 mm (*i.e.* an immersed surface of 12 mm^2) in 1 mL of organic solvent or IL previously heated to the temperature chosen for the treatment. For a surface of 12 mm^2, a theoretical maximum value of 0.026 ± 0.003 mg Pt can be recovered for El_{REF}. A gentle stirring (~ 200 rpm) was applied to prevent any contact between the magnetic bar and the electrode. All the experiments were carried out in air. At the end of the treatment time, the electrode was collected and placed vertically in a pill container with filter paper to absorb the excess of solvent. The electrode and the residual soaking solution were finally stored in closed vials for further characterizations.

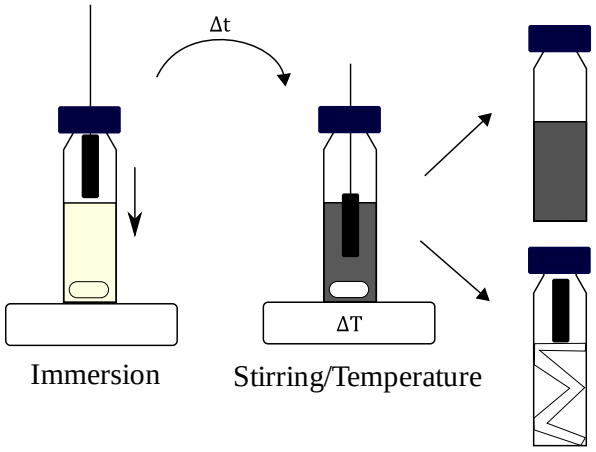

Figure 1. Experimental protocol for the extraction of Pt NPs from the electrode.

For each experiment, the electrodes used were systematically characterized by optical emission spectrometry with inductively coupled plasma (ICP-OES) and scanning electron microscopy (SEM) to determine the efficiency extent of the Pt extraction and have indications on the delamination and possible expansion of the electrode. Transmission electron microscopy (TEM) was used to characterize the residual solutions, in particular the size distribution of the Pt NPs dispersed in the liquid.

Optical emission spectrometry with inductively coupled plasma ICP-OES. The pristine and electrodes used were weighed precisely and then treated in a mixture of aqua regia type acids (1: 1 mixture of 4 M nitric acid and 4 M hydrochloric acid), this medium

was then placed in a digester micro-onde Multiwave 3000 Anton Paar, which treats the mixtures in temperature and pressure so that the platinum was completely dissolved in the medium. ICP-OES analysis was then performed on an ICP-OES 725 Agilent spectrometer.

Electron microscopy characterization. Scanning electron microscopy (SEM) measurements were performed on a JEOL XL 30. Transmission electron microscopy (TEM) characterizations were performed on a 120 kV Philips CM120. High resolution transmission electron microscopy (HRTEM) and Scanning Transmission Electron Microscopy- High Angle Annular Dark Field (STEM HAADF) images were obtained with a JEOL 2100F 200 kV microscope and a Gatan Digital Micrograph software to process the images. For each IL, a drop of the solution obtained after treatment of the electrode was placed on a copper grid. The IL in excess was then wiped off with filter paper to obtain only a very thin layer of liquid, thus allowing the characterization of any nanoparticles present in the medium. To establish an average nanoparticle sizes, at least 150 nanoparticles were counted.

Contact Angle. Contact angle measurements were performed on carbon (HOPG) and platinum platelets with the different ILs by sessile drop method using a Digidrop-GBX instrument goniometer. The advancing contact angles were measured over a timeframe of 30 seconds.

NMR spectroscopy. ^{1}H and ^{31}P NMR spectra of ILs were recorded on a Bruker Avance II 300 MHz spectrometer. Chemical shifts were measured relative to residual ^{1}H resonances in CD_2Cl_2 and ^{31}P chemical shifts were referenced to external 85% H_3PO_4 at $\delta = 0.00$ ppm.

III. Results and Discussion

In order to get deeper understanding of the mechanisms involved in the extraction of Pt from the catalytic layer (CL) of MEAs, a large panel of ILs with varied cations and anions composition was selected: *with the C_1C_4Im or C_1C_2Im cation:* $C_1C_4ImNTf_2$, C_1C_2ImTCM, $C_1C_4ImN(CN)_2$, C_1C_4ImOTf, C_1C_4ImAc and C_1C_4ImCl; with the cation P_{66614}: $P_{66614}NTf_2$, $P_{66614}N(CN)_2$, $P_{66614}TCM$, $P_{66614}Cl$, $P_{66614}Br$; with the anion NTf_2: $C_1C_1C_4ImNTf_2$, and with the anion $N(CN)_2$: $N_{4441}N(CN)_2$.

These ILs present a large panel of physicochemical properties (viscosity, surface tension, water solubility limit or molar volume) and different Kamlet-Taft parameters *i.e.* H-acceptor ability of the anion (β). Finally, the surface tension value γ (mN/m) of ILs and

the determination of their contact angle values with carbon surface (*vide infra*) could be informative on the wettability of the ILs on carbon support, which should favor the extraction of the Pt NPs. It is also worth noting that some of these anions are coordinating, and could therefore contribute to the stabilization of Pt NPs after their leaching into the IL.

In this part, a thorough screening of thirteen different ILs (Table 3) has been carried out to investigate how their structural composition as well as their physico-chemical properties may affect the extent of Pt extraction, and their ability to stabilize detached nanoparticles. The most promising Ils allowing the most efficient leaching of isolated Pt NPs in the solution have then be selected for further optimization.

Table 3. Physicochemical properties and ($\%Pt_{Ext.}$) of selected ionic liquids.

C_1C_4Im	**Anion**	**X_w max. (ref.)**	**β (51-52)**	**V_m (nm^3) (50)**	**γ (mN/m) (ref)**	($\%Pt_{Ext.}$)
1	NTf_2	0.24 (55)	0.25	295	33 (59)	6
2	OTf	1 (56)	0.49	208	35.5 (61)	23
3	TCM*	0.85 (55)	0.54	187	47.9 (60)	65
4	$N(CN)_2$	1 (56)	0.64	198	46.5 (61)	64
5	Cl	1 (56)	0.83	167	48.2 (61)	39
6	Ac	1 (57)	1.2	190	36.4 (62)	57
P_{66614}						
7	NTf_2	0.09 (58)	1.24 (53)	714	29.3 (65)	15
8	TCM	0.52 (56)	n	637	35.1 (61)	45
9	$N(CN)_2$	0.51 (55)	1.36 (53	616	31.7 (65)	34
10	Cl	0.83 (55)	1.56 (53)	587	30.6 (63)	78
11	Br	0.68 (58)	1.57 (53)	594	29.3 (64)	74
N_{4441}						
12	$N(CN)_2$	0.8 (56)	0.73 (54)	300	X	29
$C_1C_1C_4Im$						
13	NTf_2	0.19 (57)	0.24	310	37.4 (61)	12

X_w max.: maximal volume fraction of water in ILs forming a single phase; β: Kamlet-Taft coefficient (H-acceptor); $V_{m:}$ molar volume; γ: surface tension at 25 °C; *C_1C_2ImTCM. ($\%Pt_{Ext.}$): The Pt extraction from El_{REF} was carried out at 120 °C during 18 h.

III.1 Preliminary IL screening – General trends

Taking into account that ILs at room temperature have different viscosity and for meaningful comparison, the temperature of extraction was set, after optimization, at 120 °C, in order to both increase the fluidity of the ILs tested,(66) and to have viscosity in same range of values *e.g.* at 120 °C η(C_1C_4ImAc) and η(C_1C_4ImN$(CN)_2$) are equal to 9 and 4 mPa.s respectively, while at 25 °C their viscosity values are 485 and 29 mPa.s., respectively.(67,68) Moreover, the slow wettability kinetics on carbon electrodes results from combined effect of high ILs viscosity and electrodes porosity. Consequently, in order to optimize both the wetting and extraction step, the reaction time was set to 18 h.(28,69)

First, the pristine electrode El_{REF} was treated with the selected ILs at 120 °C for 18 h as described in the experimental section (Figure 1). The percentage of platinum extracted ($\%Pt_{Ext.}$) by the different ILs was determined by ICP-OES and reported in Tables 3 and Table S1 (Supporting Information). For all ILs, a darker color was observed at the end of the reaction with or without the presence of the electrode as shown in Table S2 (Supporting Information). This coloration may result from a partial degradation of ILs. The analysis of the ^{31}P, ^{13}C and ^{1}H NMR spectra of these media before and after treatment showed no notable modification of the spectra (Figures S1-S8), Supporting Information). The proportion of IL degraded under these treatment conditions was estimated to be less than 1% by mass, therefore negligible, which allows further IL recyclability.

From the in-depth study of the results reported in Table 3 and Table S1 (Supporting Information), some general trends can be established: i) For both cations C_1C_4Im and P_{66614}, the ($\%Pt_{Ext}$) was found to depend on the nature of the anion, and regardless of its nature, generally the phosphonium based ILs extracted more Pt than imidazolium ones, ii) with NTf_2^- anion, regardless of the nature of the associated cation, the ($\%Pt_{ext}$) was the lowest, suggesting that hydrophilic ILs should enhance the ($\%Pt_{Ext}$)), iii) depending on the nature of the ILs, a more or less marked expansion of the catalytic layer could be observed by SEM analysis of the electrode after treatment at 120 °C during 18 h; a total delamination of the electrode was observed only for P_{66614}Cl.

ILs based on imidazolium cation as extractant

With ILs based on imidazolium cation associated with NTf_2^-, TCM^-, $N(CN)_2^-$, OTf^-, Ac^- and Cl^-, the percentage of extracted platinum ($\%Pt_{Ext.}$) from El_{REF} varied from 6 to 65 % depending on the nature of the anion (Table 3, Entries 1 to 6).The evolution of ($\%Pt_{Ext.}$)

according to the nature of ILs could be correlated both to the β-factor (Figure S9a (Supporting Information)), hydrophilicity (Xw_{max}, Table 3) of the anion, and to the surface tension of ILs γ(mN/m) (Figure S9b (Supporting Information)). Hence, except for C_1C_4ImCl, the higher these three data values are, the better ($\%Pt_{Ext.}$) is (Table 3), leading to the following order $C_1C_4ImNTf_2$ < C_1C_4ImOTf < C_1C_4ImAc < C_1C_2ImTCM ~ $C_1C_4ImN(CN)_2$.

The TEM images of the IL suspensions after treatment, Table S1 (Supporting Information) showed that C_1C_2ImTMC, $C_1C_4ImNTf_2$, C_1C_4ImOTf, C_1C_4ImAc and $C_1C_4ImN(CN)_2$ led to a few isolated Pt NPs [mean size of ~ 3 - 5 nm] in IL suspension *i.e.* detached from the carbon support but the majority of Pt NPs were still supported onto the carbon agglomerates issued from the CL. In contrast, in C_1C_4ImCl, numerous isolated Pt NPs [mean size ~ 2 -3 nm] in suspension in IL were observed as a result of both a strong coordination of Cl^- onto Pt NPs surface making easier their leaching, and their higher stabilization in solution avoiding their aggregation.(70)

ILs based on phosphonium P_{66614} cation as extractant

For ILs based on P_{66614} cation, ($\%Pt_{Ext}$) varied as follows: $P_{66614}NTf_2$ << $P_{66614}N(CN)_2$ < $P_{66614}TCM$ < $P_{66614}Cl$~ $P_{66614}Br$ (Table 3, entries 7 to 11). As for the imidazolium based ILs, the ($\%Pt_{Ext}$) variations are governed by the nature of the anion *i.e.* they have an upward trend as the β-factor value and the water volume fraction Xw_{max} increase (Figures S10a and S10b respectively (Supporting Information)), and a decay for larger molar volume Vm of the IL (Table 3).

Despite a hydrophobic nature limiting their solubility in water to 0.5 mol/mol, it is interesting to note that the P_{66614}^+ cation characterized by a large molar volume - long alkyl chains- and a high viscosity when associated with any anion, excepted with $N(CN)_2^-$ yielded a ($\%Pt_{Ext.}$) superior than its imidazolium analogues. Accordingly, these results may be the consequence of a better wetting of the carbon surface by ILs based on P_{66614}^+ cation compared to imidazolium derived ILs, *vide infra*.(28,29)

As for C_1C_4ImCl, $P_{66614}Cl$ and $P_{66614}Br$ led to numerous isolated Pt NPs in the solution. These NPs have a similar mean size (~2 nm) to those observed on the pristine

electrode, so their properties are likely to be preserved during the treatment (Table S1, Supporting Information).

ILs based on the same anion as extractant

The (%Pt_{Ext}) was evaluated with two groups of ILs based on the same anion NTf_2^- and $N(CN)_2$. For all ILs based on NTf_2^- anion, $C_1C_4ImNTf_2$, $C_1C_1C_4ImNTf_2$, and $P_{66614}NTf_2$, the (%Pt_{ext}) was low ≤ 15 %, and varied as: $C_1C_4ImNTf_2$ (6 %) < $C_1C_1C_4ImNTf_2$ (12 %) < $P_{66614}NTf_2$ (15 %) inversely to the molar volume *e.g.* $C_1C_1C_4ImNTf_2$ (V_m = 310 nm^3) extracted twice as much Pt NPs from the CL than $C_1C_4ImNTf_2$ (V_m = 295 nm^3), and in the case of $P_{66614}NTf_2$ exhibiting the highest molar volume (V_m = 714 nm^3), (%Pt_{ext}) was optimal, (Table 3 entries 1, 7, 13). Moreover, for these ILs, no isolated Pt NPs in suspension were observed on the TEM images of the solution after treatment (Table S1, Supporting Information).

With $C_1C_4ImN(CN)_2$, $N_{4441}N(CN)_2$ and $P_{66614}N(CN)_2$, the (%Pt_{Ext}), following the order: $N_{4441}N(CN)_2$ (29 %) < $P_{66614}N(CN)_2$ (34 %) < $C_1C_4ImN(CN)_2$ (64 %), was significantly higher than those obtained with all ILs based on the NTf_2^- anion which could be related to higher β Kamlet-Taft coefficient, hydrophilic character X_{wmax} and surface tension γ of the $N(CN)_2^-$ anion than the NTf_2^- anion. The higher (%Pt_{Ext}) value measured with $C_1C_4ImN(CN)_2$ could account for its greater hydrophilicity (X_{wmax} = 1) compared to $P_{66614}N(CN)_2$. (X_{wmax} = 0.51) Note that in this case a smaller IL molar volume could favor the (%Pt_{Ext}): $P_{66614}N(CN)_2$ [V_m = 616 nm^3, (%Pt_{Ext}) = 34] *vs.* $C_1C_4ImN(CN)_2$ [V_m = 198 nm^3, %Pt_{ext} = 64] (Table 3, entries 4, 9, 12). With these ILs based on the $N(CN)_2$ anion, some Pt NPs [size in a range of 4-7 nm] were present in IL solution, most of Pt NPs remained anchored on dispersed surface carbon (Table S1, Supporting Information).

III.2 Influence of the IL wettability on the Pt extraction performance

The above results highlight that several physico-chemical properties of ILs control the platinum extraction with the first step related to the wettability of the electrode by the ILs. In order to identify the role of this factor, we determined the values of the contact angles of a range of imidazolium- and phosphonium-based ILs on Highly Ordered Pyrolytic Graphite (HOPG) used as a carbon black model component of the catalytic layer

to avoid IL absorption by electrode porosity and contact angle determination issues due to surface irregularities (Table 4).

Table 4. Contact angle values of $C_1C_4ImNTf_2$, C_1C_4ImAc, C_1C_4ImTCM, $P_{66614}TCM$ and $P_{66614}Cl$ on HOPG coal.

IL	Contact angle (deg.)	$(\%Pt_{Ext})^a$
C_1C_4ImAc	46 ± 4	57
C_1C_2ImTCM	42 ± 5	65
$C_1C_4ImNTf_2$	27 ± 1	6
$P_{66614}TCM$	0 (in 4 s.)	45
$P_{66614}Cl$	0 (in 3 s.)	78

[a] %Pt extraction after treatment of the El_{REF} in ionic liquids at 120 °C for 18 h, before washing with CH_3CN.

In Table 4, we observed firstly, that among the imidazolium-based ILs, $C_1C_4ImNTf_2$ had the smallest contact angle and despite this strong IL/HOPG interaction,(31) the ($\%Pt_{Ext}$) was very low (6 %) *vs.* 57 % and 65 % respectively for C_1C_4ImAc and C_1C_2ImTCM. Secondly, as reported in literature, P_{66614} based ILs exhibited much lower contact angles, close to zero degree, indicating rapid spreading and high interactions of these liquids over the carbon surface within a few seconds.(28,29) However, the wettability factor is not an universal indicator of extraction efficiency. Indeed, in spite of a better wettability, $P_{66614}TCM$ has a lower ($\%Pt_{Ext}$) than C_1C_2ImTCM.. Again, it could be argued that, for the same anion, the molar volume of IL could influence the extraction performance.

The highest ($Pt_{Ext}.\%$) should be related, not only to the ILs physico-chemical properties and optimal wettability but also to the fact, that at 120 °C after 18 h, $P_{66614}Cl$ was capable of disaggregating and dispersing the CL affording a total delamination of the electrode (Table SI, Supporting Information).

III.3 Influence of IL on coal dispersion

The carbon black (Vulcan XC 72R) of pristine electrode was made up of spherical primary particles of several tens of nm in diameter grouped into aggregates which themselves form agglomerates of the order of a micrometer, Table 1.To compare the capacity of ILs to disperse and to stabilize carbon black, an analysis of the size of the carbon particles extracted after treatment at 120 °C for 18 h was carried out and monitored by TEM experiments. In C_1C_2ImTCM and C_1C_4ImAc, a large particles size distribution was

observed with an average diameter around ~ 120 nm, Figure 2A-B, while it was ~ 90 nm for $P_{66614}TCM$, Figure 5C, and ~50 nm with a narrow distribution for $P_{66614}Cl$, Figure 2D. This dispersion by IL of the carbon black where the Pt NPs are initially deposited could thus be one of the key conditions to access to Pt, favoring its extraction.

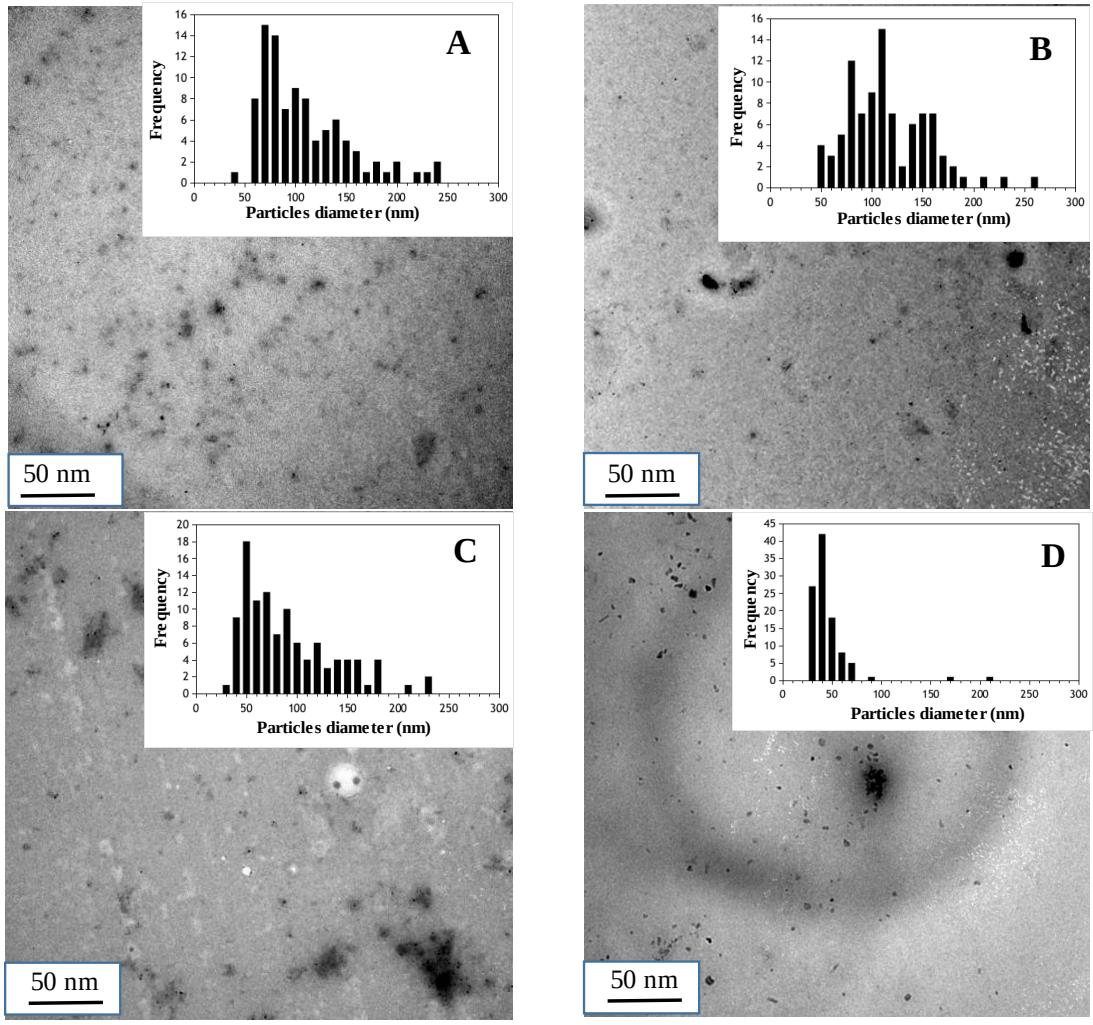

Figure 2. TEM images and histograms of carbon particles of the CL suspension in A) C_1C_2ImTCM, B) C_1C_4ImAc, C) $P_{66614}TCM$, D) $P_{66614}Cl$ after treatment of the pristine electrode during 18 h at 120 °C.

III.4 Influence of the electrode washing on the Pt extraction performance

To avoid any Pt extraction unrelated to the action of the IL, the above results were obtained without washing the electrode after treatment. However, as some ILs are very viscous and can have a strong affinity with the different elements contained in the electrode, a significant amount of IL may remain on the electrode after treatment, which could underestimate the extraction percentages. We have therefore chosen to introduce a washing step prior to any characterization. In order to ensure that the organic solvents used did not

interfere in the extraction process, their impact on the stability of the electrode was studied at room temperature. Toward this end, the electrodes were immersed (3x4 mm^2) for 1 h at room temperature (~ 25 °C) in 1 mL of polar solvent, (ultrapure water (H_2O), acetonitrile (CH_3CN), isopropanol (iPrOH), dimethylsulfoxide (DMSO), ethanol (EtOH) and dimethylacetamide (DMAc).

With H_2O, CH_3CN, iPrOH and DMSO, no change in appearance of the solution and no delamination of the electrode were observed (Table S3, Supporting Information). With EtOH and DMAc, however, a gray suspension was obtained and the SEM images indicate a significant delamination of the catalytic layer. Due to the high solubility of ILs in CH_3CN and the absence of significant changes in the surface of the electrode, this solvent was chosen to remove residual ILs from the electrode after the treatment.

The washing procedure consists of immersing the electrode after treatment in a pill container containing 1 mL of acetonitrile for 30 to 60 seconds. For certain ILs ($P_{66614}NTf_2$, $P_{66614}Br$, $P_{66614}Cl$ and C_1C_4ImCl), this resulted in a dispersion of black particles. For these ILs, the washing with CH_3CN induced an increase of ($Pt_{Ext.}$) ~ 20 %, achieving in the case of $P_{66614}Br$ and $P_{66614}Cl$ a total extraction of the initial Pt present on the electrode. This result confirms that residual IL containing dispersed Pt NPs was present on the electrode, but did not change the general trend, Figure 3. Taken together, it seems that the extent of (%Pt_{Ext}) for pristine electrode correlates with the nature of the anion which controls hydrophilicity, β Kamlet-Taft coefficient, and molar volume of the IL. However, many deviations from these general trends have been highlighted throughout our studies. Consequently, none of these factors can predict in a reliable way the extractive power of ILs. Likewise, although in some cases a linear correlation could be established between (%Pt_{Ext}) and β Kamlet-Taft coefficient of the anion, numerous anomalies were observed, in particular with the anions Cl^-, $(CN)_2N^-$, and AcO^- . However, the surface tension γ (mN/m) and the hydrophilicity of the ILs, which determine their wettability on the carbon surface were shown to be crucial parameters to reach high (%$Pt_{Ext.}$) values. Thus, ILs derived from P_{66614}^+ generally have a higher (%$Pt_{Ext.}$) probably related to their higher wettability on the carbon surface but also to their higher ability to disperse the carbon support into smaller carbon particles. Finally, isolated and stabilized Pt NPs (2 to 4 nm mean size) in the solution have only been detected with IL associated with Cl^- anions

whereas with others ILs, the Pt NPs were agglomerated or remained onto the carbon agglomerates detached from the CL.

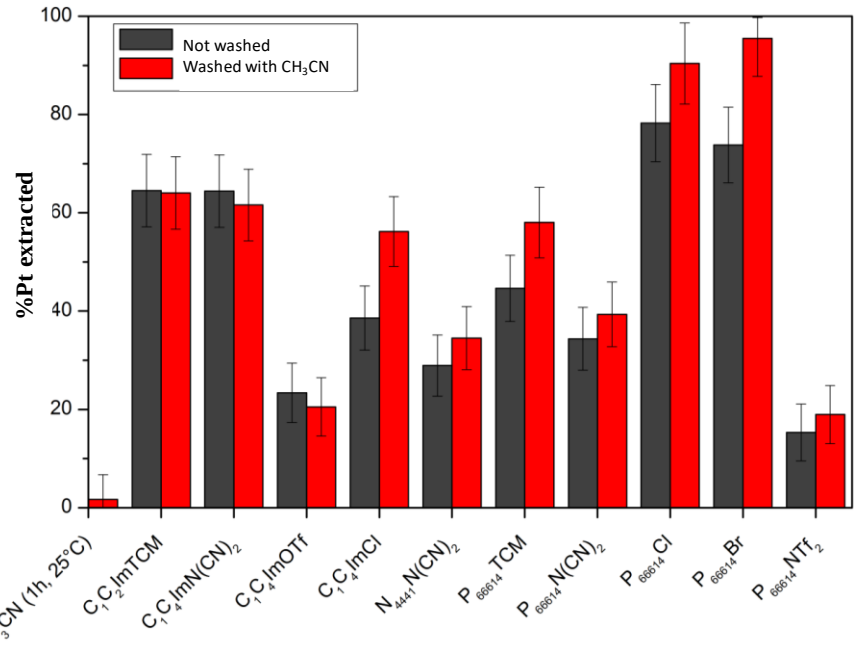

Figure 3. Influence of washing with acetonitrile on the %Pt extraction after treatment of the El_{REF} in ionic liquids at 120 °C for 18 h. Each measurement is independent.

It emerges from these screening studies that the IL allowing the most efficient leaching of isolated Pt NPs into the solution was $P_{66614}Cl$, in addition to being inexpensive commercially available and very thermally and chemically stable.(71).

III.5 Optimization of (%$Pt_{Ext.}$) with the model system (El_{REF} / $P_{66614}Cl$)

With $P_{66614}Cl$, a more in-depth study was therefore undertaken, using the electrode manufactured at the CEA, the reference electrode El_{REF} ,whose platinum loading ~ 0.22 mg $Pt.cm^{-2}$ is close to the electrodes currently marketed (Table 1). The procedure is described in Figure 1 and the (%$Pt_{Ext.}$) was determined by ICP-OES. The evolution of (%$Pt_{Ext.}$) as a function of time and temperature was studied. On the other hand, tests aiming at simplifying the process and/or reducing the cost (energy or product prices) have been carried out.(72)

Influence of the temperature and reaction time

The evolution of (%$Pt_{Ext.}$) as a function of time was performed, in air, at three different temperatures: 25, 80 and 120 °C (Figure 4). At 25 °C, the (%Pt_{Ext}) rate was slower and increased with time. After 18 h of immersion, (%$Pt_{Ext.}$) was ~ 30 % and reached 60 %

after 168 h (Figure 4, left). At 80 °C after 1 h, the (%$Pt_{Ext.}$) reached 32 % then increased with time to ~ 78 % in 18 h and ~ 88 % in 172 h (Figure 4, middle). A complete delamination of the CL could therefore be achieved at 80 °C for long immersion time. However, the color of the solution remained yellow and clear after 18 h.

At 120 °C after 1 h, the (%$Pt_{Ext.}$) reached 66 %, and increased to ~ 78 % after 6 h. Then, it remained steady between 6 and 18 h (Figure 4, right). The color of the solution was brown and cloudy after 4 h of immersion.

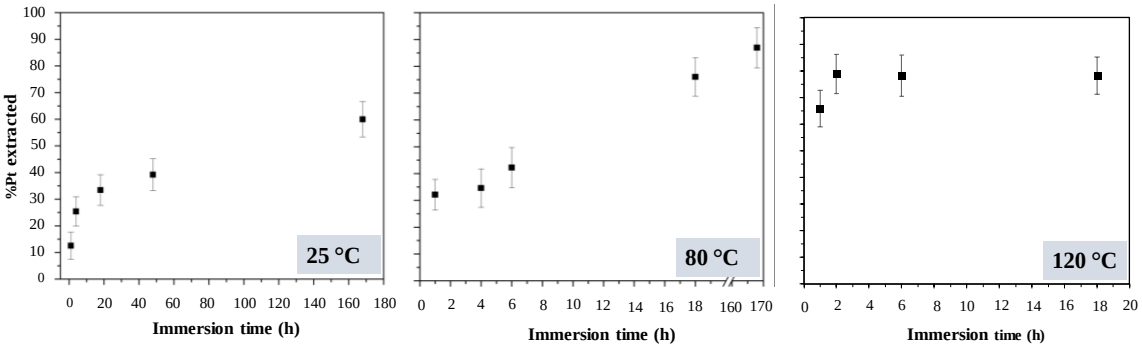

Figure 4. Evolution of (%$Pt_{Ext.}$) as a function of immersion time in $P_{66614}Cl$ performed at 25 , 80 and 120 °C, in air.

Influence of the platinum concentration

The previous tests were carried out with electrode surfaces of 12 mm^2 affording a final Pt concentration of ~20 µgPt / mL, when (%$Pt_{Ext.}$) was greater than 80 %. To allow a more realistic comparison with industrial processes, the effect of increasing Pt concentration in 1 mL of IL was explored to better delineate the limits of our process. As shown in Table 5, when three samples of 100 mm^2 (~ 8 times larger) were immersed successively in the same volume of $P_{66614}Cl$ (1mL) for 24 h at 80 °C, the values of (%$Pt_{Ext.}$) of the three samples were similar to those obtained with a smaller surface affording a final concentration of 520 µgPt /mL_{LI}. This observation suggests that the extent of (%$Pt_{Ext.}$) did not change as the Pt NPs becomes more concentrated in $P_{66614}Cl$.

Table 5. (%$Pt_{ext.}$) in 1mL of $P_{66614}Cl$ at 80 °C, 24 h, in air, with 3 sample of 1 cm^2.

Sample	**(%$Pt_{ext.}$) (ICP-OES)**	**Surface**
reference	80 ± 7 %	12 mm^2
1	66 ± 7 %	100 mm^2
2	86 ± 8 %	100 mm^2
3	84 ± 8	100 mm^2

Extracted platinum nanoparticles characterization

Under these experimental conditions, Scanning Transmission Electron Microscopy- High Angle Annular Dark Field (STEM HAADF) images, carried out directly in the IL solution, showed that Pt NPs were either attached to the carbonaceous support (Figure 5, left) or isolated in the IL with an average diameter ~ 2.7 nm (Figures 5, middle). The HRTEM images showed that the isolated Pt NPs in IL exhibit a well-defined crystallinity and the analysis of the Fourier transform allowed to obtain well-defined Bragg spots in the reciprocal space whose distances between planes correspond to metallic platinum (Figures 5, right).(73)

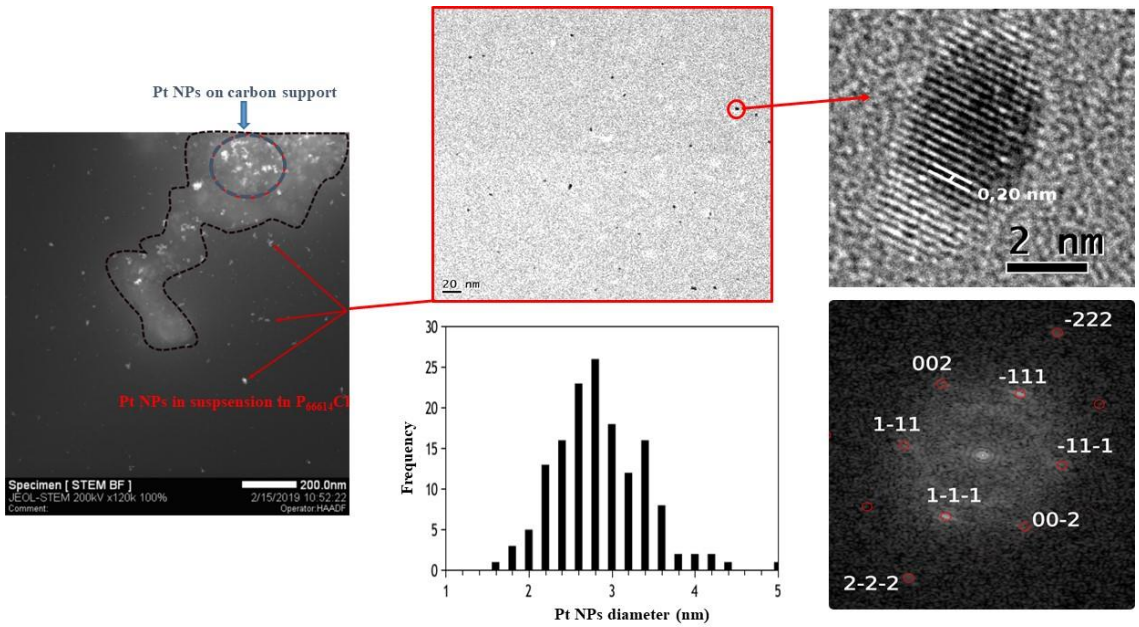

Figure 5. STEM HAADF images of the dispersion in $P_{66614}Cl$ from 1 cm^2 of El_{REF} immersed during 18 h at 80 °C (left); TEM images of Pt NPs suspended in $P_{66614}Cl$ (concentration of 0.5 mg_{Pt}/cm^2) and Pt NPs diameter histogram (middle); HRTEM images of Pt NPs and Fourier transform allowing the determination of the plan 101, mesh parameter of 3.923 Å corresponding to Pt(0).(73)

On the other hand, after treatment at 120 °C for 18 h in $P_{66614}Cl$, the Pt NPs are detached from the carbonaceous support with an average diameter of 3.3 nm very slightly greater than that observed at 80 °C (Figure 6).

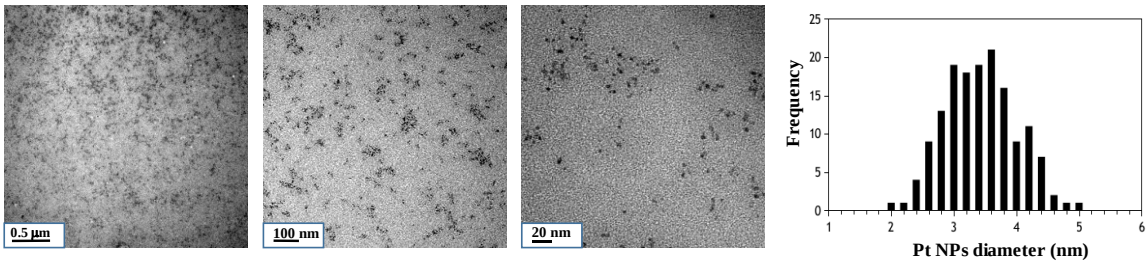

Figure 6. TEM images of the suspension in $P_{66614}Cl$ from 1 cm² of El_{REF} after immersion during 18 h at 120 °C and Pt NPs diameter histogram.

In conclusion, at 80 or 120 °C, during 18 h, in air, $P_{66614}Cl$ yielded (%$Pt_{Ext.}$) ~ 90 % after introducing a step of washing with CH_3CN of the CL. The value of (%$Pt_{Ext.}$) did not significantly change when the Pt concentration was increased by a factor of 8 by simply increasing the immersed electrode surface. The metallic Pt NPs are totally detached from the carbon surface and have an average diameter of 3.3 nm, a size similar to the initial one, thanks to the stabilizing effect of $P_{66614}Cl$.

Evolution of (%$Pt_{ext.}$) in $P_{66614}Cl$/ H_2O mixture

Knowing that $P_{66614}Cl$ is very hygroscopic and that the experiments were run in air, the effect of increased quantity of water on (%$Pt_{Ext.}$) has been studied (Figure 7). The reaction temperature was settled at 80 °C to avoid water ebullition. Moreover, the addition of water significantly reduced the viscosity of the system (from ~ 1900 mPa.s to ~ 100 mPa.s at 25 °C and 15 mPa.s at 80 °C), when the IL was saturated with water *i.e.* for a molar fraction of 0.82 at 25 °C and around 0.9 at 80 °C. (58,74)

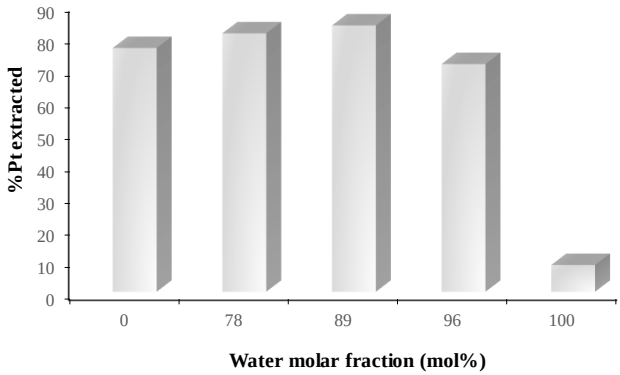

Figure 7. Evolution of (%$Pt_{ext.}$) as a function of water molar ratio added to $P_{66614}Cl$. Immersion conditions: 18 h at 80 °C. Each experiment is independent.

Data from Figure 7 revealed that at 80 °C for 18 h, water alone allowed only very low platinum extraction (~ 7 %) while the introduction of water in $P_{66614}Cl$ led to only a

very slight change in (%$Pt_{Ext.}$), varying from 76 % to 83 % up to a water molar ratio x_w equal to 89 mol% (~20 % by volume). Up to a molar fraction of 0.9, the IL is saturated with water, the extraction rate dropped sharply.

With $P_{66614}Cl$, under optimized experimental conditions, the presence of water was shown to have a positive effect on (%$Pt_{Ext.}$). Indeed, the water decreases the viscosity of the IL at 25 °C, (58,74) thus avoiding the washing step with an organic solvent, and facilitating the separation of Pt NPs between the IL and aqueous phases, hence making this process less expensive and safer. (75)

Effect of the variation of the ionomer level of the catalytic layer

All previous experiments were performed on a single type of electrode (EL_{ref}). To develop a versatile process of Pt NPs extraction different compositions of electrodes have been tested with different Nafion ionomer proportions.

Table 6. Main characteristic of the electrode surfaces (12 mm^2) used in this work.

Electrode	**support**	**Pt wt%**	**i/C**	**Loading (mg Pt.cm^{-2})**	**Thickness CL (µm)**	**Size Pt-NPs (nm)**	**(%$Pt_{ext.}$)**
El_{REF}	GDL	34.3	0.67	0.22 ± 0.03	~ 10	3.0 ± 0.6	90.4 ± 8.3
El2	GDL	*id*	0.3	0.24	*id.*	*id.*	53.02 ± 5.8
EL3	GDL	*id*	0.94	0.22	*id.*	*id.*	91.2 ± 6.6
EL4	ETFE	26.5	0.66	0.17	*id.*	*id.*	99.2 ± 6
Commercial Electrode $El_{Com.}$	GDL	54.5	0.94	1.729 ± 0.021	~ 30	3.4 ± 0.8	96.5 ± 3.3

ETFE stands for ethylene tetrafluoroethylene. *id.* stands for identical.

Table 6 shows the value of (%$Pt_{Ext.}$) in $P_{66614}Cl$ during a treatment at 120 °C for 18 h for electrode samples of 12 mm^2 containing different proportion of ionomer in the catalytic layer (i/C: defined as the mass of ionomer mixed with the mass of the catalyst powder). The loading in platinum was similar, except for the commercial electrode $El_{com.}$. The nature of the support of the catalytic layer did not significantly change the results since (%$Pt_{Ext.}$) remained close to 100 % for a layer of carbon paper (GDL) as well as for a layer of ethylene tetrafluoroethylene (ETFE). However, the (%$Pt_{Ext.}$) increased from 50 % for i/C = 0.3 to more than 90 % when i/C = 0.66. These results highlight that the amount of ionomer therefore has a major role on (%$Pt_{Ext.}$) implying that the ionomer could intervene in the mechanism of platinum extraction.

IV. Conclusion

A safer and greener process than those usually based on pyro-hydrometallurgical technologies was developed to recover the Pt catalyst from MEAs without the need of calcination step and dissolution of Pt NPs in acidic and corrosive medium. In our approach, we sought to use ILs as both extractant to recover the Pt directly in its metallic form as well as stabilization agent of the detached Pt NPs. A large panel of ILs with different physico-chemical properties and varied cation/anion composition have been selected to study the influence of ILs and associated processing parameters on the extraction of platinum from the catalytic layer of MEAs. Variable extraction results were obtained depending on the nature and properties of ILs. After optimization, we have been able to obtain a process, which not only results in the extraction of Pt up to > 90 % of the Pt initially present on the catalytic layer, but also allows in a single step to detach the Pt NPs from its carbon support. The process implemented is simple and consists of immersing the electrode in trihexyltetradecylphosphonium chloride ($P_{66614}Cl$) during 6 hours at 120 °C in air with gentle magnetic stirring followed by washing the electrode with acetonitrile at room temperature. A dispersion of Pt NPs of a size close to that initially present in the catalytic layer and detached from their carbon supports was observed with this specific IL, thus facilitating their direct reuse. Note that this process was not impacted by the presence of water below 10 % of the total volume in the $P_{66614}Cl$, which allows the implementation of this process under air. In addition, during the screening study, other ILs providing satisfactory Pt extraction around 60-70 % led to the extraction of carbon black in the form of aggregates or primary particles, which makes it possible to consider the separation and reuse of the different elements of the catalytic layer for specific applications.

Contact angle measurements on carbon model material (HOPG) revealed that ILs could interact with all the components of the active layer. Among the different interactions allowing the best results in terms of extraction, the Nafion-IL interaction seems to be of particular importance. The variation of the ionomer content in the catalytic layer was indeed directly correlated to the efficiency of extraction. Therefore, the interaction and wettability of ILs with the different component of the CL and particularly with the ionomer (swelling) should be further studied to deepen our understanding of the mechanism of platinum extraction by ionic liquids. A detail study using the best ILs candidates, in particular $P_{66614}Cl$, will be presented in the part 2 of this series of publications through small angle X-ray scattering and wide angle X-ray diffraction techniques.

Supporting Information

Evolution of the %Pt extracted in different ILs, SEM analysis of the electrode and TEM images of the IL suspension, evolution of the color of ionic liquids in the presence or absence of electrodes after treatment at 120 °C, evolution of the color of different organic solvents and SEM images of the electrode after immersing the treated electrode at 120 °C, ^{1}H and ^{31}P NMR spectra of ILs before and after treatment at 120 °C, Evolution of the %Pt extracted in ILs based on imidazolium and phosphonium cations as a function of the physicochemical properties of ILs.

Acknowledgement

New Technologies for Energy Grant (CEA/C2P2 Platform), MEARIL Project.

References

(1) James, B. D., Huya-Kouadio, J. M., Houchins, C., DeSantis, D. A. Mass production cost estimation for direct H_2 PEM fuel cell systems for transportation applications: . *Report to the DOE Fuel Cell Technologies Program*. **2018 Update.** https://www.energy.gov/sites/prod/files/2019/12/f70/fcto-sa-2018-transportation-fuel-cell-cost-analysis.pdf.
(2) Kamarudin, S. K., Hashim, N., Materials, morphologies and structures of MEAs in PEMFCs, *Renew. Sust. Energ. Rev.*, **2012**, 162494-2515.
(3) Zhang, X., Li, H., Yang, J., Lei, Y., Wang, C., Wang, J., Tang, Y., Mao, Z., Recent advances in Pt-based electrocatalysts for PEMFCs , *RSC Adv*., **2021**, 11, 13316–13328.
(4) EUROPEAN COMMISSION, *Report from the Commission to the European Parliament, the Council, the European Economic and Social Committee and the Committee of the Regions on the implementation of the Circular Economy Action Plan*, available at https://ec.europa.eu/environment/circular-economy/ (Accessed on February 26, **2020**).
(5) a) Duclos, L., Chattot, R., Dubau, L., Thivel, P.-X., Mandil, G., Laforest, V., Bolloli, M., Vincent, R., Svecova, L., Closing the loop: life cycle assessment and optimization of a PEMFC platinum-based catalyst recycling process, *Green Chem*., **2020**, 22, 1919–1933. b) Valente, A., Iribarren, D., Dufour, J., End of life of fuel cells and hydrogen products: From technologies to strategies, *Int. J. Hydrog. Energy Volume*, **2019,** 44, 38, 20965-20977.
(6) a) Duclos, L., Svecova, L., Laforest, V., Mandil, G., Thivel, P.-X., Process development and optimization for platinum recovery from PEM fuel cell catalyst, *Hydrometallurgy*, **2016**, 160, 79-89. b) DOE, Recovery of Platinum Metals From PEMFCs - Market Research Study **2022** available at https://science.osti.gov/-/media/sbir/pdf/Market-Research/AMO---Recovery-of-Platinum-September-2022-Public.pdf.
(7) Rzelewska-Piekut, M., Paukszta, D., Regel-Rosocka, M., Hydrometallurgical recovery of platinum group metals from spent automotive converters, *Physicochem. Probl. Miner. Process*, **2021**, 57, 83-94.
(8) Sharma, R., Nielsen, K. R., Lund, P. B., Simonsen, S. B., Grahl-Madsen, L., Andersen, S. M., Sustainable Platinum Recycling through Electrochemical Dissolution of Platinum Nanoparticles from Fuel Cell Electrodes, *ChemElectroChem*, **2019**, 6, 4471–4482.
(9) Shore, L., Robertson, A. B., Shulman, H. S., Fall, M. L., Process for recycling components for a PEM fuel cell membrane electrode assembly, US 2006/0237034A1, **2006**.
(10) Coleman, R. J., Ralph, T. R., Haig, S., Plechkova, N. V., Process for recovery of perfluorosulfonic acid ionomer for fuel cell membrane or catalyst ink., WO2016156815A1, **2016**.
(11) Koehler, J., Zuber, R., Binder, M., Baenisch, V., Lopez, M., Process for recycling fuel cell components containing precious metals, US20080064771A1, **2008**.
(12) Dietz-Cory, M. L., Hawkins, A., Metal Ion Extraction With Ionic Liquids, Handbooks in Separation Science, Elsevier, **2020**, Chapter 18, pp 539-564 https://doi.org/10.1016/B978-0-12-816911-7.00018-9.
(13) Wasserscheid, P., Welton, T., *Ionic Liquids in Synthesis*, 2d Edition Wiley-VCH, Weinheim, **2008**.
(14) Diallo, A.O., Len, C. Morgan, A. B., Marlair, G., Revisiting physico-chemical hazards of ionic liquids, *Sep. Purif. Tech.*, **2012**, 97, 228-234.

(15) Mokhodoeva, O., Shkine, V., Maksimov, V., Dzhenlod, R., Spivakov, B., Recovery of platinum group metals using magnetic nanoparticles modified with ionic liquids, *Sep. Purif. Tech.*, **2020**, 248, 117049.
(16) Endres, F., Abbott, A. P., MacFarlane, D., *Electrodeposition from Ionic Liquids*. Wiley-VCH Weinheim. **2017.**
(17) Abbott, A. P., Frisch, G., Hartley, J., Ryder, K. S., Processing of metals and metal oxides using ionic liquids, *Green Chem*., **2011**, 13, 471-481.
(18) Binnemans, K., Lanthanides and Actinides in Ionic Liquids, *Chem Rev*., **2007**, 107, 2592-2614.
(19) Billard, I., Ouadi, A., Gaillard, C., Liquid–liquid extraction of actinides, lanthanides, and fission products by use of ionic liquids: from discovery to understanding, *Anal Bioanal. Chem.*, **2011**. 400, 1555-1566.
(20) Nguyen, V. T., Lee, J., Chagnes, A., Kim, M., Jeong, J., Cote, G., Highly selective separation of individual platinum group metals (Pd, Pt, Rh) from acidic chloride media using phosphonium-based ionic liquid in aromatic diluent , *RSC Adv.*, **2016**, 6, 62717-62728.
(21) Firmansyah, M.L., Kubota, F., Yoshida, W., Goto, M., Application of a Novel Phosphonium-Based Ionic Liquid to the Separation of Platinum Group Metals from Automobile Catalyst Leach Liquor, *Ind. Eng. Chem. Res*., **2019**, 58, 3845−3852.
(22) Svecova, L., Papaïconomou, N., Billard I., Rh(III) Aqueous Speciation with Chloride as a Driver for Its Extraction by Phosphonium Based Ionic Liquids, *Molecules*, **2019**, 24, 1391.
(23) Fajar, A.T.N., Hanada, T., Goto M., Recovery of platinum group metals from a spent automotive catalyst using polymer inclusion membranes containing an ionic liquid carrier, *J. Membrane Sci.*, **2021**, 629, 119296.
(24) Lanaridi, O., Sahoo, A. R., Limbeck, A., Naghdi, S., Eder, D., Eitenberger, E., ʾCsendes, Z., Schnürch, M., K., Toward the Recovery of Platinum Group Metals from a Spent Automotive Catalyst with Supported Ionic Liquid Phases, *ACS Sustain. Chem. Eng.*, **2021**, 9, 375–386.
(25) Matsumoto H., in *Electrochemical Aspects of Ionic Liquids* (Ed.: H. Ohno), John Wiley & Sons, Hoboken, **2005**, pp. 35–54.
(26) Balva, M., Legeai, S., Leclerc, N., Billy, E., Meux, E., Environmentally Friendly Recycling of Fuel Cell Membrane Electrode Assemblies by Using Ionic Liquids, *ChemSusChem*., **2017** 10, 2922-2935.
(27) Huang, J.-F. & Chen, H.-Y., Heat-assisted electrodissolution of platinum in an ionic liquid, *Angew. Chem. Int. Ed.*, **2012**, 51, 1684–1688.
(28) Zhang, W., Jiang, S., Sun, J., Wu, Z., Qin, T., Xi, X., Wettability of coal by room temperature ionic liquids, *Int. J. Coal Prep. Util.*, **2021**, 41, 418-427. https://doi.org/10.1080/19392699.2018.1488692.
(29) Painter, P., Pulati, N., Cetiner. R., Dissolution and dispersion of coal in ionic liquids, *Energ. Fuel.* **2010**, 24, 1848–53.
(30) Lei, Z. P., Hu, Z. Q., Zhang, H., Han, L., Shui, H., Ren, S., Wang, Z., Kang, S., Pan. C., Pyrolysis of lignite following low temperature ionic liquid pretreatment, *Fuel*, **2016**, 166,124-29.
(31) Bordes, E., Douce, L., Quitevis, E. L., Pádua, A. A. H., Costa Gomes, M. F., Ionic liquids at the surface of graphite: Wettability and structure, *J. Chem. Phys.*, **2018**, 148, 193840.

(32) Lu, J., Yang, J.-X., Wang, J., Lim, A., Wang, S., Loh, K. P., Nanoribbons, Nanoparticles, and Graphene by the Exfoliation of Graphite in Ionic Liquids, *ACS Nano*, **2009**, 3 ,2367–2375.
(33) Fampiou, I., Ramasubramaniam, A., Binding of Pt Nanoclusters to Point Defects in Graphene: Adsorption, Morphology, and Electronic Structure, *J. Phys. Chem. C*, **2012,** 116, 6543-6555.
(34) Brunello, G. F., Lee, J. H., Lee, S. G., Choi, J. I., Harvey, D., Jang, S. S., Interactions of Pt nanoparticles with molecular components in polymer electrolyte membrane fuel cells: multi-scale modeling approach, *RSC Adv.*, **2016**. 6, 69670-69676.
(35) Feng, C., Wang, J., Cheng, Y., He, P., Liew, K. M., Diffusion mechanism of platinum nanoclusters on well-aligned carbon nanotubes, *RSC Adv.*, **2014**, 105, 60711-60719.
(36) Schneider, W. B., Benedikt, U., Auer, A. A., Interaction of Platinum Nanoparticles with Graphitic Carbon Structures: A Computational Study, *ChemPhysChem*, **2013**, 14, 2984-2989.
(37) Dupont, J., Scholten, J.D., On the structural and surface properties of transition-metal nanoparticles in ionic liquids, *Chem. Soc. Rev.*, **2010**, 39, 1780–1804.
(38) Kraynov, A., Müller, T. E., Concepts for the Stabilization of Metal Nanoparticles in Ionic Liquids, in *Applications of ionic liquids in science and technology*, Ed. Handy S.T., INTECH open, Rijeka **2011**, Chapter 12.
(39) Katsyuba, S. A., Zvereva, E. E., Yan, N., Yuan, X., Kou, Y., Dyson, P. J. Rationalization of Solvation and Stabilization of Palladium Nanoparticles in Imidazolium-Based Ionic Liquids by DFT and Vibrational Spectroscopy, *ChemPhysChem*, **2012** , 13, 1781-1790.
(40) Zvereva, E. E., Grimme, S., Katsyuba, S. A., Ermolaev, V. V., Arkhipova, D. A., Yan, N., Miluykov, V. A., Sinyashin, O. G., Aleksandrov, A., Solvation and stabilization of palladium nanoparticles in phosphonium-based ionic liquids: a combined infrared spectroscopic and density functional theory study, *Phys. Chem. Chem. Phys*., **2014**, 16, 20672-20680.
(41) Podgorsek, A., Pensado, A. S., Santini, C. C., Costa Gomes, M. F., Padua, A. A. H., Interaction Energies of Ionic Liquids with Metallic Nanoparticles: Solvation and Stabilization Effects, *J. Phys. Chem. C*, **2013**, 117, 3537–3547.
(42) Pensado, A. S., Padua, A. A. H., Solvation and Stabilization of Metallic Nanoparticles in Ionic Liquids, *Angew. Chem. Int. Ed.*, **2011**, 50, 8683-8687.
(43) Doyle, M., Choi, S. K., Proulx, G., High-Temperature Proton Conducting Membranes Based on Perfluorinated Ionomer Membrane-Ionic Liquid Composites, *J. Electrochem. Soc*., **2000**, 147, 34– 37.
(44) Sun, J., Jordan, L. R., Forsyth, M., MacFarlane, D. R., Acid-Organic base swollen polymer membranes, *Electrochim. Acta*, **2001**, 46, 1703-1708.
(45) Izak, P., Hovorka, S., Bartovsky, T., Bartovska, L., Crespo, J. G., Swelling of polymeric membranes in room temperature ionic liquids, *J. Membrane Sci*., **2007**, 296, 131-138.
(46) Sood, R., Iojoiu, C., Espuche, E., Gouanvé, F., Gebel, G., Mendil-Jakani, H., Lyonnard, S., Jestin, J., Proton Conducting Ionic Liquid Doped Nafion Membranes: Nano-Structuration, Transport Properties and Water Sorption, *J. Phys. Chem. C*, **2012**, 116, 46, 24413–24423.
(47) Sood, R., Iojoiu, C., Espuche, E., Gouanvé, F., Gebel, G., Mendil-Jakani, H., Lyonnard, S., and Jestin, J., Comparative Study of Proton Conducting Ionic Liquid Doped

Nafion Membranes Elaborated by Swelling and Casting Methods: Processing Conditions, Morphology, and Functional Properties, *J. Phys. Chem. C*, **2014**, 118, 14157–14168.
(48) da Trindad, L. G., Zanchet, L., Borba, K. M. N., Souza, J. C., Leite, E. R., Martini, E. M. A, Effect of the doping time of the 1-butyl-3 methylimidazolium ionic liquid cation on the Nafion membrane proprieties, *Int. J. Energy Res*., **2018**, 42, 3535–3543.
(49) Danyliv, O., Martinelli, A., Nafion/Protic Ionic Liquid Blends: Nanoscale Organization and Transport Properties, *J. Phys. Chem. C*, **2019**, 123, 14813-14824.
(50) Marcus, Y., Ionic and molar volumes of room temperature ionic liquids, *J. Mol. Liq.*, **2015**, 209, 289-293.
(51) Lungwitz, R., Strehmel, V., Spange, S., The dipolarity/polarisability of 1-alkyl-3-methylimidazolium ionic liquids as function of anion structure and the alkyl chain length, *New J. Chem.*, **2010** 34, 1135-1140.
(52) Ab Rani, M. A., Brant, A., Crowhurst, L., Dolan, A., Lui, M., Hassan, N.H., Hallett, J. P., Hunt, P.A., Niedermeyer, H., Perez-Arlandis, J.M., Schrems, M., Welton, T., Wilding, R., Understanding the polarity of ionic liquids, *Phys. Chem. Chem. Phys*., **2011**, 13, 16831-16840.
(53) Padró, J. M., Reta, M., Solvatochromic parameters of imidazolium-, hydroxyammonium-, pyridinium- and phosphonium-based room temperature ionic liquids, *J. Mol. Liq.*, **2016**, 213, 107-114.
(54) Thielemann, G., Spange, S., Polarity of tetraalkylammonium-based ionic liquids and related low temperature molten salts, *New J. Chem.*, **2017,** 41, 8561-8567.
(55) Freire, M. G., Santos, L. M. N. B. F., Fernandes, A. M., Coutinho, J. A. P., Marrucho, I. M., An overview of the mutual solubilities of water–imidazolium-based ionic liquids systems, *Fluid Ph. Equilibria*, **2007**, 261, 449-454.
(56) Troshenkova, S. V., Sashina, E. S., Novoselov, N. P., Arndt, K.-F., Jankowsky, S., Structure of ionic liquids on the basis of imidazole and their mixtures with water, *Russian J. Gen. Chem.*, **2010**, 80, 106-111.
(57) Martins, M. A. R., Neves C. M. S. S., Kurniaa, K. A., Santos, L. M. N. B. F., Freire, M. G., Pinho, S. P., Coutinho, J. A. P., Analysis of the isomerism effect on the mutual solubilities of bis(trifluoromethylsulfonyl)imide-based ionic liquids with water, *Fluid Ph. Equilibria*, **2014**, 381, 28-35.
(58) Freire, M. G., Carvalho, P. J., Gardas,R. L., Santos, L. M. N. B. F., Marrucho, I. M., Coutinho, J. A. P., Solubility of Water in Tetradecyltrihexylphosphonium-Based Ionic Liquids, *J. Chem. Eng. Data*, **2008,** 53, 2378-2382.
(59) Jin, H., O'Hare, B., Dong, J., Arzhantsev, S., Baker, G. A., Wishart, J. F., Benesi, A. J., Maroncelli, M., Physical Properties of Ionic Liquids Consisting of the 1-Butyl-3-Methyl imidazolium Cation with Various Anions and the Bis(trifluoromethylsulfonyl) imide Anion with Various Cations, *J. Phys. Chem. B*, **2008**, 112, 81-92.
(60) Martino, W., de la Mora, J. F., Yoshida, Y., Saito, G., Wilkes, J., Surface tension measurements of highly conducting ionic liquids, *Green Chem.*, **2006**. 8, 390-397.
(61)Tariq, M., Freire, M. G., Saramago, B., Coutinho, J. A. P., Lopes, J. N. C., Rebelo, L. P. N., Surface tension of ionic liquids and ionic liquid solutions, *Chem. Soc. Rev.*, **2012**, 41, 829-868.
(62) Almeida, H. F. D., Passos, H., Lopes-da-Silva, J. A., Fernandes, A. M., Freire, M. G., Coutinho, J. A. P., Thermophysical Properties of Five Acetate-Based Ionic Liquids, *J. Chem. Eng. Data*, **2012**, 573005-3013.

(63) Almeida, H. F. D. Lopes-da-Silva, J. A. , Freire, M. G. , Coutinho, J. A. P. « Surface tension and refractive index of pure and water-saturated tetradecyltrihexylphosphonium-based ionic liquids, *J. Chem. Thermodyn.*, **2013**. 57, 372-379.
(64) Manic, M. S., Macedo, E. A., Najdanovic-Visak, V., Trihexyl(tetradecyl)phosphonium bromide: Liquid density, surface tension and solubility of carbondioxide, *Fluid Ph. Equilibria*, **2012,** 324, 8-12.
(65) Blanco, D., Bartolomé, M., Ramajo, B., Viesca, J. L., González, R., Hernández Battez, A., Wetting Properties of Seven Phosphonium Cation-Based Ionic Liquids, *Ind. Eng. Chem. Res.*, **2016**, 55, 9594-9602.
(66) Okoturo, O. O., VanderNoot, T. J., Temperature dependence of viscosity for room temperature ionic liquids, *J. Electroanal. Chem.*, **2004**, 568, 167-181.
(67) Yoshida, Y., Baba, O., Saito, G., Ionic Liquids Based on Dicyanamide Anion: Influence of Structural Variations in Cationic Structures on Ionic Conductivity, *J. Phys. Chem. B*, **2007**, 111, 4742-4749.
(68) Fendt, S., Padmanabhan, S., Blanch, H. W., Prausnitz, J. M.,Viscosities of Acetate or Chloride-Based Ionic Liquids and Some of Their Mixtures with Water or Other Common Solvents, *J. Chem. Eng. Data*, **2011**, 56 31-34.
(69) Bolimowska, E., Morales-Ugarte, J. E., Roault, H., Santos-Pena J., Santini, C. C., Benayad, A., Influence of the vinylene carbonate on the wetting and interface chemical structure of doped ionic liquid electrolyte at porous graphite surface, *J Phys Chem C*, **2017**, 121, 16166-16173.
(70) Zhao, S., Ren, Y., Lu, W., Wang, J., Yin, W., A theoretical investigation of the interaction between small Pd particles and 1-butyl-3-methyl imidazolium ionic liquids with Cl^-, $BF4^-$ and $PF6^-$ anions, *Phys. Chem. Chem. Phys.*, **2012,** 14, 13444-13451.
(71) Gonçalves, F. A. M. M., Costa, C. S. M. F., Ferreira, C. E., Bernardo, J. C. S., Johnson, I., Fonseca, I. M. A., Ferreira, A. G. M., Pressure–volume–temperature measurements of phosphonium-based ionic liquids and analysis with simple equations of state, *J. Chem. Thermodyn.*, **2011**, 43, 914-929.
(72) Billy E, Coudray M, Dufaud V, Haumesser P-H, Mendil-Jakani H, Santini C, Procédé de récupération de particules de platinoïde contenues dans un support électriquement isolant, patent CEA-CNRS EP3815762 A1, 2021.
(73) Salzemann, C., Kameche, F., Ngo, A.-T., Andreazza, P., Calatayud M., Petit, C., Platinum and platinum based nanoalloys synthesized by wet chemistry, *Faraday Discuss.*, **2015**, 181, 19-36.
(74) Neves, C. M. S. S., Carvalho, P. J., Freire, M. G., Coutinho, J. A. P., Thermophysical properties of pure and water-saturated tetradecyltrihexylphosphonium-based ionic liquids, *J. Chem. Thermodyn.*, **2011,** 43, 948-957.
(75) Cui, P., He, H., Chen, D., Liu, H., Zhang, S., Yang, J., Phase Transfer of Noble Metal Nanoparticles from Ionic Liquids to an Organic/Aqueous Medium, *Ind. Eng. Chem. Res*., **2014**, 53, 15909-15916.

Table of Contents